Rotation-Torsion Interaction in the Ground State Microwave Spectrum of Trans-gauche Ethylnitrite

Ch. Keussen and H. Dreizler

Abteilung Chemische Physik im Institut für Physikalische Chemie der Universität Kiel

Z. Naturforsch. **46 a,** 590–594 (1991); received March 30, 1991

We investigated a small rotation-torsion interaction in the microwave spectrum of trans-gauche ethylnitrite, CH_3CH_2ONO. We found the difference between the two lowest energy levels of the torsion around the C–O bond axis to be 24.8(8) kHz. The high resolution of microwave Fourier transform (MWFT) spectroscopy was necessary to measure the resulting small splittings.

Introduction

Several investigations were made on the microwave spectrum of ethylnitrite in recent years. Turner [1] assigned the spectra of three conformers called cis-trans, cis-gauche, and trans-gauche ethylnitrite. They are shown in Figure 1. Endo et al. [2] recorded the spectra of some istopomers and determined partial structures. In 1988 we published the ground state quadrupole coupling constants of all three conformers [3] determined by microwave Fourier transform (MWFT) spectroscopy. We found an additional splitting of the *c*-type transitions of trans-gauche ethylnitrite. Turner [1] found a similar, but much larger splitting of the *c*-type transitions of the named conformer in an excited state of the torsion around the C–O bond axis. This splitting is caused by the interaction between the overall rotation and the tunneling motion through the barrier separating the two equivalent gauche-conformations. The splitting in the ground torsional state should have the same reason. To confirm this hypothesis, further research had to be done.

Experimental

Ethylnitrite was purchased from Fa. Merck-Schuchardt, Darmstadt, in a purity of 85% and distilled under low pressure for further purification. The measurements were made with waveguide MWFT spectrometers in the frequency range from 3.8 to 40 GHz [4–8] at pressures between 0.025 and 0.2 Pa and temperatures between −30 and −55 °C. We focused our attention on recording additional *c*-type transitions to gain more information on the rotation-torsion interaction.

The Fourier transformation of a transient emission signal into the frequency domain causes line shape deformations, especially in the case of narrow multipletts [9]. To eliminate these overlap effects, the frequencies of the transitions were determined by a least squares fit of the time domain signal [10]. Because this fit program was improved since our last publication on ethylnitrite [3], all transitions given there were refitted to gain more accurate hyperfine frequencies. We focused our attention on measuring additional *c*-type transitions with their torsional hyperfine structure. A total of 5 *a*- and 29 *c*-type transitions was measured. A list of all transitions is given in Table 1. For an example see Fig. 3 of [3]. To calculate the hypothetical center frequencies we used the quadrupole coupling

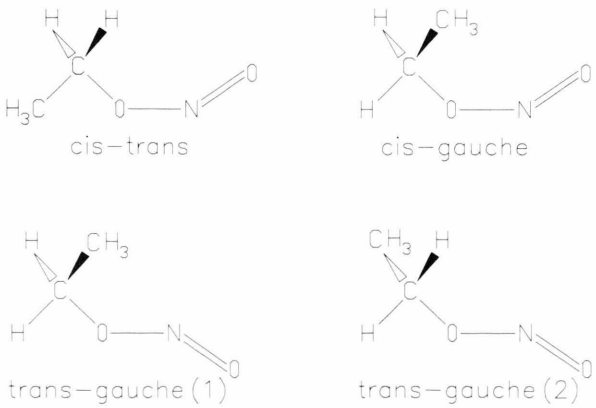

Fig. 1. Rotational isomers of ethylnitrite.

Reprint requests to Prof. Dr. H. Dreizler, Institut für Physikalische Chemie der Universität Kiel, Ohlshausenstr. 40, W-2300 Kiel 1, Germany.

0932-0784 / 91 / 0700-0590 $ 01.30/0. – Please order a reprint rather than making your own copy.

Table 1. Rotational transitions of trans-gauche ethylnitrite. ν_{obs}: measured frequency [MHz], ν_c: hypothetical unsplit line frequency [MHz] calculated by adding the hfs-splittings to the frequencies of the components, δ_c: deviation of the centrifugal distortion calculation [MHz].

$J_{K_-K_+} \leftarrow J'_{K'_-K'_+}$	$v \leftarrow v'$	$F \leftarrow F'$	ν_{obs}	ν_c	δ_c
$3_{21} \leftarrow 2_{20}$	0←0	4←3	16 103.018		
	1←1	3←2	16 103.203	16 103.057	−0.004
		2←1	16 102.927		
$3_{22} \leftarrow 2_{21}$	0←0	4←3	16 099.808		
	1←1	3←2	16 100.004	16 099.850	0.002
		2←1	16 099.714		
$4_{04} \leftarrow 3_{03}$	0←0				
	1←1		21 454.494	21 454.494	0.003
$4_{04} \leftarrow 3_{12}$		5←4	6 112.748		
	1←0	4←3	6 113.942	6 113.049	−0.004
		3←2	6 112.359		
		5←4	6 112.700		
	0←1	4←3	6 113.892	6 113.001	0.000
		3←2	6 11.306		
$4_{14} \leftarrow 3_{13}$	0←0	5←4	21 208.315		
	1←1	4←3	21 208.366	21 208.350	0.002
		3←2	21 208.413		
$5_{15} \leftarrow 4_{14}$	0←0	6←5	26 508.382		
	1←1	5←4		26 508.410	−0.002
		4←3	26 508.446		
$7_{17} \leftarrow 7_{07}$		8←8	13 267.201		
	1←0	7←7	13 268.247	13 267.506	−0.004
		6←6	13 267.048		
		8←8	13 267.148		
	0←1	7←7	13 268.194	13 267.452	−0.005
		6←6	13 266.994		
$7_{07} \leftarrow 6_{15}$		8←7	21 176.484		
	1←0	7←6	21 177.763	21 176.851	−0.002
		6←5	21 176.278		
		8←7	21 176.433		
	0←1	7←6	21 177.712	21 176.800	0.002
		6←5	21 176.227		
$8_{18} \leftarrow 8_{08}$		9←9	12 815.276		
	1←0	8←8	12 816.302	12 815.579	−0.001
		7←7	12 815.144		
		9←9	12 815.221		
	0←1	8←8	12 816.248	12 815.525	−0.002
		7←7	12 815.089		
$9_{19} \leftarrow 9_{09}$		10←10	12 322.745		
	1←0	9←9	12 323.742	12 323.040	0.003
		8←8	12 322.633		
		10←10	12 322.670		
	0←1	9←9	12 323.688	12 322.985	0.002
		8←8	12 322.581		
$10_{1\,10} \leftarrow 10_{0\,10}$		11←11	11 794.981		
	1←0	10←10	11 795.952	11 795.274	0.000
		9←9	11 794.882		
		11←11	11 794.926		
	0←1	10←10	11 795.898	11 795.218	−0.001
		9←9	11 794.827		
$11_{1\,11} \leftarrow 11_{0\,11}$		12←12	11 237.834		
	1←0	11←11	11 238.768	11 238.115	0.003
		10←10	11 237.749		
		12←12	11 237.780		
	0←1	11←11	11 238.712	11 238.059	0.002
		10←10	11 237.691		

Table 1 (continued)

$J_{K_-K_+} \leftarrow J'_{K'_-K'_+}$	$v \leftarrow v'$	$F \leftarrow F'$	ν_{obs}	ν_c	δ_c
$12_{1\,12} \leftarrow 12_{0\,12}$		13←13	10 657.434		
	1←0	12←12	10 658.331	10 657.709	0.002
		11←11	10 657.359		
		13←13	10 657.379		
	0←1	12←12	10 658.274	10 657.652	0.001
		11←11	10 657.302		
$13_{1\,13} \leftarrow 13_{0\,13}$		14←14	10 060.178		
	1←0	13←13	10 061.030	10 060.437	−0.001
		12←12	10 060.116		
		14←14	10 060.116		
	0←1	13←13	10 060.974	10 060.382	0.000
		12←12	10 060.054		
$14_{1\,14} \leftarrow 14_{0\,14}$		15←15	9 452.531		
	1←0	14←14	9 453.340	9 452.780	0.000
		13←13	9 452.472		
		15←15	9 452.472		
	0←1	14←14	9 453.280	9 452.722	−0.002
		13←13	9 452.411		
$15_{1\,15} \leftarrow 15_{0\,15}$		16←16	8 840.924		
	1←0	15←15	8 841.686	8 841.159	−0.002
		14←14	8 840.869		
		16←16	8 840.869		
	0←1	15←15	8 841.629	8 841.104	0.001
		14←14	8 840.814		
$16_{1\,16} \leftarrow 16_{0\,16}$		17←17	8 231.587		
	1←0	16←16	8 232.297	8 231.808	0.001
		15←15	8 231.532		
		17←17	8 231.532		
	0←1	16←16	8 232.240	8 231.753	0.004
		15←15	8 231.480		
$16_{2\,15} \leftarrow 16_{1\,15}$		17←17	36 558.829		
	1←0	16←16	36 660.021	36 559.177	−0.004
		15←15	36 558.908		
		17←17	36 558.744		
	0←1	16←16	36 559.934	36 559.092	0.001
		15←15	36 558.823		
$17_{1\,17} \leftarrow 17_{0\,17}$		18←18	7 630.393		
	1←0	17←17	7 631.056	7 630.598	−0.002
		16←16	7 630.354		
		18←18	7 630.334		
	0←1	17←17	7 630.998	7 630.540	−0.002
		16←16	7 630.294		
$18_{1\,18} \leftarrow 18_{0\,18}$		19←19	7 042.741		
	1←0	18←18	7 043.359	7 042.931	−0.002
		17←17	7 042.708		
		19←19	7 042.682		
	0←1	18←18	7 043.298	7 042.873	−0.001
		17←17	7 042.647		
$19_{1\,19} \leftarrow 19_{0\,19}$		20←20	6 473.417		
	1←0	19←19	6 473.983	6 473.592	0.000
		18←18	6 473.386		
		20←10	6 473.358		
	0←1	19←19	6 473.923	6 473.533	−0.001
		18←18	6 473.327		
$19_{2\,18} \leftarrow 19_{1\,18}$		20←20	33 265.585		
	1←0	19←19	33 626.671	33 625.922	0.002
		18←18	33 625.521		
		20←20	33 625.486		
	0←1	19←19	33 626.578	33 625.827	0.006
		18←18	33 625.430		

Table 1 (continued)

$J_{K_-K_+} \leftarrow J'_{K'_-K'_+}$	$v \leftarrow v'$	$F \leftarrow F'$	ν_{obs}	ν_c	δ_c
		21←21	5 926.508		
	1←0	20←20	5 927.023	5 926.668	0.000
		19←19	5 926.481		
$20_{1\,20} \leftarrow 20_{0\,20}$		21←21	5 926.449		
	0←1	20←20	5 926.965	5 926.608	0.002
		19←19	5 926.422		
		21←21	32 538.124		
	1←0	20←20	32 539.191	32 538.461	0.001
		19←19	32 538.071		
$20_{2\,19} \leftarrow 20_{1\,19}$		21←21	32 538.028		
	0←1	20←20	32 539.097	32 538.364	0.004
		19←19	32 537.970		
		22←22	5 405.340		
	1←0	21←21	5 405.810	5 405.485	0.001
		20←20	5 405.317		
$21_{1\,21} \leftarrow 21_{0\,21}$		22←22	5 405.281		
	0←1	21←21	5 405.752	5 405.426	0.000
		20←20	5 405.259		
		23←23	4 912.464		
	1←0	22←22	4 912.888	4 912.595	0.000
		21←21	4 912.444		
$22_{1\,21} \leftarrow 22_{0\,21}$		23←23	4 912.406		
	0←1	22←22	4 912.830	4 912.537	0.000
		21←21	4 912.386		
		23←23	30 269.910		
	1←0	22←22	30 270.959	30 270.237	−0.008
		21←21	30 269.862		
$22_{2\,21} \leftarrow 22_{1\,21}$		23←23	30 269.806		
	0←1	22←22	30 270.856	30 270.133	−0.006
		21←21	30 269.753		
		25←25	27 904.838		
	1←0	24←24	27 905.842	27 905.152	0.003
		23←23	27 904.769		
$24_{2\,23} \leftarrow 24_{1\,23}$		25←25	27 904.735		
	0←1	24←24	27 905.732	27 905.048	−0.003
		23←23	27 904.692		
		26←26	26 697.339		
	1←0	25←25	26 698.315	26 697.644	0.002
		24←24	26 697.296		
$25_{2\,24} \leftarrow 25_{1\,24}$		26←26	26 697.225		
	0←1	25←25	26 698.202	26 697.531	0.004
		24←24	26 697.183		
		27←27	25 479.733		
	1←0	26←26	25 480.689	25 480.031	0.003
		25←25	25 479.695		
$26_{2\,25} \leftarrow 25_{1\,25}$		27←27	25 479.619		
	0←1	26←26	25 480.572	25 479.916	−0.001
		25←25	25 479.580		
		28←28	24 257.192		
	1←0	27←27	24 257.156	24 257.481	0.001
		26←26	24 258.119		
$27_{2\,26} \leftarrow 27_{1\,26}$		28←28	24 257.071		
	0←1	27←27	24 257.035	24 257.360	−0.001
		26←26	24 257.997		
		29←29	23 035.009		
	1←0	28←28	23 035.903	23 035.288	−0.001
		27←27	23 034.977		
$28_{2\,27} \leftarrow 28_{1\,27}$		29←29	23 034.881		
	0←1	28←28	23 035.779	23 035.160	−0.002
		27←27	23 034.847		

Table 1 (continued)

$J_{K_-K_+} \leftarrow J'_{K'_-K'_+}$	$v \leftarrow v'$	$F \leftarrow F'$	ν_{obs}	ν_c	δ_c
		30←30	21 818.558		
	1←0	29←29	21 819.418	21 818.824	−0.002
		28←28	21 818.525		
$29_{2\,28} \leftarrow 29_{1\,28}$		30←30	21 818.419		
	0←1	29←29	21 819.285	21 818.689	0.002
		28←28	21 818.388		
		31←31	20 613.203		
	1←0	30←30	20 614.040	20 613.460	−0.002
		29←29	20 613.174		
$30_{2\,29} \leftarrow 30_{1\,29}$		31←31	20 613.065		
	0←1	30←30	20 613.903	20 613.322	0.002
		29←29	20 613.034		

constants from [3]. Since they are determined with sufficient accuracy, no effort was made to improve them further.

Theoretical Background

To fit the rotation-torsion interaction we assumed the molecule to be rigid with exception of the large amplitude internal torsion around the C–O bond axis. In Fig. 2 one can see that this bond axis is nearly parallel to the a-principal inertia axis. To simplify the setup of the Hamiltonian we made the approximation that the torsional angular momentum couples with the a-component P_a of the total angular momentum only. It is then possible to fit the spectra of the hypothetical center frequencies to a Hamiltonian [1] in the so called reduced axis system. The potential function of the torsion is a double minimum potential shown in Figure 3. The Hamiltonian in a II^r-representation ($a=y$, $b=z$, $c=x$) can be written as follows:

$$\hat{\boldsymbol{H}} = \begin{pmatrix} \hat{\boldsymbol{H}}_{00} & \hat{\boldsymbol{H}}_{01} \\ \hat{\boldsymbol{H}}_{01} & \hat{\boldsymbol{H}}_{11} \end{pmatrix}, \tag{1a}$$

$$\hat{\boldsymbol{H}}_{00} = A_0 \hat{P}_a^2 + B_0 \hat{P}_b^2 + C_0 \hat{P}_c^2 + \hat{\boldsymbol{H}}_{cd00}\,, \tag{1b}$$

$$\hat{\boldsymbol{H}}_{11} = A_1 \hat{P}_a^2 + B_1 \hat{P}_b^2 + C_1 \hat{P}_c^2 + \hat{\boldsymbol{H}}_{cd11} + \Delta E_{01}\,, \tag{1c}$$

$$\hat{\boldsymbol{H}}_{01} = F_{01}(\hat{P}_b \hat{P}_c + \hat{P}_c \hat{P}_b)\,. \tag{1d}$$

$A_0, B_0, C_0, A_1, B_1, C_1$: rotational constants in the torsional states $v=0$, 1, respectively,

$\hat{\boldsymbol{H}}_{cd}$: Hamiltonian of the centrifugal distortion up to sixth order according to Watson's A reduction,

ΔE_0: energy difference of the two torsional states $v=0$ and $v=1$ (see Fig. 3),

F_{01}: fit parameter of the rotation-torsion interaction.

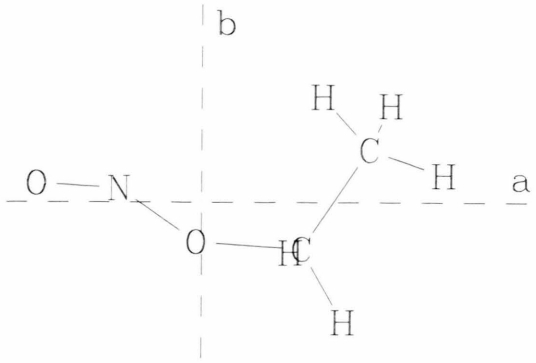

Fig. 2. Trans-gauche ethylnitrite in a projection on the *a*, *b*-principal inertia axis plane.

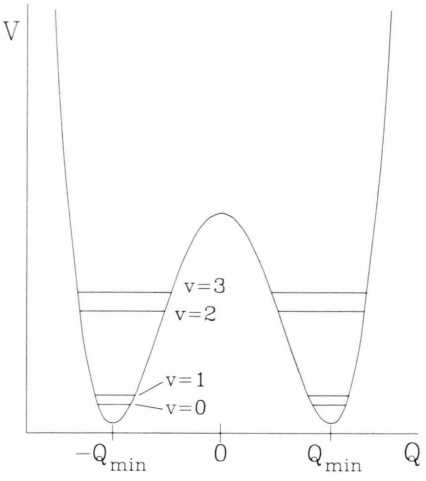

Fig. 3. Potential energy function of the symmetric double minimum potential. Q: torsional coordinate, V: potential energy.

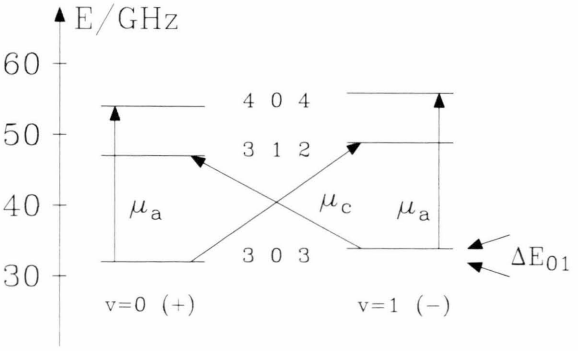

Fig. 4. Some energy levels and possible transitions of trans-gauche ethylnitrite.

Table 2. Rotational and centrifugal distortion constants written in the notation of sums and differences explained in the text. A, B, C: rotational constants, Δ_J, Δ_{JK}, Δ_K, δ_J, δ_K, Φ_J, Φ_{JK}, Φ_{KJ}, Φ_K, ϕ_J, ϕ_{JK}, ϕ_K: fourth and sixth order centrifugal distortion constants according to Watson's A-reduction, rotation-torsion interaction constants ΔE_{01}, F_{01}: explanation see text, $\varkappa$: asymmetry parameter, σ: standard deviation of the fit, standard errors in brackets, $\Delta\bar{\nu}_{exp}$: mean experimental torsion splitting, largest correlation coefficient: $(|\Delta_J, \Delta_K|) = -0.992$.

A	17 639.500 (10) MHz	Φ_{KJ}	−1.14 (30) kHz
B	2 745.031 (6) MHz	Φ_K	0.55 (17) kHz
C	2 620.852 (5) MHz	ϕ_J	43.8 (52) Hz
Δ_J	628.4 (29) kHz	ϕ_{JK}	−279. (71) Hz
Δ_{JK}	−1 979.2 (80) kHz	ϕ_K	271. (83) Hz
Δ_K	1 357.0 (48) kHz	ΔE_{01}	24.8 (8) kHz
δ_J	−313.7 (15) kHz	F_{01}	7.2 (18) kHz
δ_K	673.7 (30) kHz	ΔC	12. (2) Hz
Φ_J	−92. (11) Hz	ΔB	54. (6) Hz
Φ_{JK}	0.683 (15) kHz	$\Delta(\Delta_K)$	0.007 (9) Hz
σ:	5 kHz	$\Delta\bar{\nu}_{exp}$:	77 kHz

We assume that only the first two torsional states ($v=0, 1$ in Fig. 3) take part in the rotation-torsion interaction. The Hamiltonian (1 b), (1 c) includes the usual centrifugal distortion $\hat{H}_{cd}$ according to Watson [12]. This implies that the rigidity for vibrational degrees of freedom has been lifted by allowing small amplitude vibrations.

Only a short sketch of the development of this Hamiltonian is outlined in [11]. We therefore performed a careful step by step development of the Hamiltonian and confirmed especially that the transformation from the principal axis system of inertia to the reduced axis system is in fact a contact transformation. That means that the angular momenta components in the reduced axis system obey the normal commutation relations of quantum mechanical angular momenta and can be treated in the usual manner. Details of these rather extended considerations are given in [13].

The c-dipole moment μ_c is an odd function of the C–O torsional angle, hence c-type transitions connect the $v=0$ and $v=1$ torsional states and show a splitting of approximately twice the energy difference ΔE_{01} (see Figure 4).

The fit of the measured transitions to the Hamiltonian was carried out with a modified version of the program MALON*.

* Original written by L. Halonen, P. H. Turner, and J. Randell.

Results and Discussion

From the splittings of the *c*-type transitions (ca. 45–140 kHz) one expects the torsional energy difference ΔE_{01} to be in the range between 20 and 70 kHz. This small difference entails that the rotational and centrifugal distortion constants for both torsional states are nearly equal. The following notation is employed. For example:

$$A = \frac{A_0 + A_1}{2}, \quad \Delta A = \frac{A_0 - A_1}{2}. \tag{2}$$

When performing a centrifugal distortion analysis according to Watson up to sixth order, we have 15 independent rotational and centrifugal distortion constants for each torsional state, or, with the just given notation, 15 sums and 15 differences of them. In addition we must fit ΔE_{01} and F_{01}. Because we could not fit 32 parameters to 68 transitions independently and simultaneously, some fixing of common rotational and centrifugal distortion constants for the two torsional states was necessary. Therefore a first fit was carried out with all differences of constants fixed to zero. We then tried to improve the reproduction of the measured spectrum with different combinations of differences allowed to be nonzero and included in the fit. The best reproduction was achieved with inclusion of ΔB_v, ΔC_v, and $\Delta(\Delta_K)_v$. The results are summarized in Table 2. One can see from this Table that the energy difference ΔE_{01} is only 24.8(8) kHz. The high resolution of MWFT spectroscopy was necessary to determine such a small effect with sufficient accuracy.

Acknowledgement

We thank the members of our group for help and discussions and P. Cox for sending the original version of the program MALON. Funds of the Deutsche Forschungsgemeinschaft, Fonds der Chemie, and the Land Schleswig-Holstein are gratefully acknowledged.

[1] P. H. Turner, J. Chem. Soc. Faraday Trans. II **75,** 317 (1979).
[2] K. Endo, T. Koshiba, H. Saito, and Y. Kamura, Nippon Kagaku Kaishi **1980,** 1661,
[3] Ch. Keussen, U. Andresen, and H. Dreizler, Z. Naturforsch. **43a,** 469 (1988).
[4] G. Bestmann, H. Dreizler, H. Mäder, and U. Andresen, Z. Naturforsch. **35a,** 392 (1980).
[5] G. Bestmann, H. Dreizler, E. Fliege, and W. Stahl, J. Mol. Struct. **97,** 215 (1983).
[6] W. Stahl, G. Bestmann, H. Dreizler, U. Andresen, and R. Schwarz, Rev. Sci. Instrum. **56,** 1759 (1985).
[7] H. Ehrlichmann, J. U. Grabow, H. Dreizler, N. Heineking, R. Schwarz, and U. Andresen, Z. Naturforsch. **44a,** 751 (1989).
[8] Ch. Keussen, N. Heineking, and H. Dreizler, Z. Naturforsch. **44a,** 215 (1989).
[9] I. Merke and H. Dreizler, Z. Naturforsch. **43a,** 196 (1988).
[10] J. Haekel and H. Mäder, Z. Naturforsch. **43a,** 203 (1988).
[11] H. M. Pickett, J. Chem. Phys. **56,** 1715 (1972).
[12] W. Gordy and R. L. Cook, Microwave Molecular Spectra, 3rd ed., John Wiley & Sons, New York 1984, p. 331.
[13] Ch. Keussen, Dissertation, Kiel 1991, Chapt. II, p. 48–76.